JOURNAL OF SOLID STATE CHEMISTRY **141,** 221–228 (1998)
ARTICLE NO. SC987959

Nonstoichiometric Li-Pseudobrookite(ss) in the Li_2O-Fe_2O_3-TiO_2 System

I. E. Grey,[1] C. Li, and T. Ness

CSIRO Division of Minerals, P.O. Box 312, Clayton South, Australia 3169

Received February 6, 1998; in revised form June 4, 1998; accepted July 6, 1998

Phase equilibria in the Li_2O-Fe_2O_3-TiO_2 system were studied at 900 and 1000°C using the quenching method. Two new ternary solid solutions, based on the pseudobrookite and ramsdellite structure types, were identified and structurally characterised using Rietveld refinements of powder X-ray data. The pseudobrookite(ss) showed deviations from M_3O_5 stoichiometry towards metal-rich compositions which increased with increasing substitution of Li+Ti for Fe, from Fe_2TiO_5 to $Li_{0.81}Fe_{0.27}Ti_{2.09}O_5$ ($\equiv M_{3.17}O_5$). A neutron diffraction refinement was made on $Li_{0.81}Fe_{0.27}Ti_{2.09}O_5$, space group C*cmm*, with $a = 9.6576(2)$, $b = 3.7532(1)$, $c = 9.8820(2)$ Å. Titanium is ordered in the eightfold M2 site while lithium, together with minor iron and titanium, is ordered in the four-fold M1 site. The excess lithium (0.17 Li per formula unit) was located in interstitial sites in the structure, having square-pyramidal coordination. A local-ordering model is presented which involves Li_3 clusters with Li-Li = 2.3 Å.

INTRODUCTION

Phase relations in the Li_2O-Fe_2O_3-TiO_2 system at 800 and 900°C were reported by Yau and Hughes (1). The only ternary phases they identified were members of the spinel solid solution, $LiFe_5O_8$-$Li_4Ti_5O_{12}$, and of the rocksalt-type solid solutions between $LiFeO_2$ (cubic) and Li_2TiO_3 (monoclinic). Pseudobrookite was shown as a point phase on their diagrams, Fe_2TiO_5, with no solid solution extension due to lithium incorporation. However, in a study on the reactions of ilmenite and titania slag with lithium borates, Easteal and Udy (2) prepared iron titanate phases having the pseudobrookite structure which were shown to contain significant amounts of lithium.

As part of a general study on the influence of additives on ilmenite upgrading (3, 4) we investigated the reactions of lithium-containing additives with ilmenite under oxidising conditions. In contrast to the results of Yau and Hughes (1) we found that lithium readily entered the pseudobrookite structure to form an extended solid solution. This led to a study of the stability and phase relations of the pseudobrookite(ss) in the Li_2O-Fe_2O_3-TiO_2 system. The study showed that the pseudobrookite(ss) compositions were significantly displaced from the M_3O_5 stoichiometric line towards lithia-rich compositions. The structural aspects of lithium incorporation into pseudobrookite were investigated using Rietveld refinement of powder X-ray diffraction and neutron diffraction data. We report here the results of the phase equilibria and structural studies.

[1]Corresponding author.

EXPERIMENTAL

Phase Equilibria

Phase equilibria in air were investigated by the quenching method. Starting materials for powder preparations were Fisher certified titania (anatase form) and analytical grade hematite and lithium carbonate, all of small particle size and all dried prior to the experiments. The $LiO_{0.5}$-$FeO_{1.5}$-TiO_2 phase field was restricted to compositions containing >33 mol% TiO_2, <45 mol% $LiO_{1.5}$, and <67 mol% $FeO_{1.5}$. Mixtures of the starting materials corresponding to compositions within this phase field were weighed and thoroughly mixed then heated at 800°C to decompose the carbonate. They then underwent repeated heatings in air at temperatures of 900°C or 1000°C for periods of typically 20 h with intermediate grindings until PXRD patterns on the quenched samples showed a single phase (or failed to do so). Portions of the single phase products were analysed for iron, titanium, and lithium using atomic emission spectroscopy (ICP-AES). Accurate lattice parameters for the single phase products were obtained by Rietveld analysis of ball-milled products using X-ray intensity data.

Particular attention was given to checking for lithia volatilisation. Careful weight loss experiments on the most lithia-rich compositions used in this study showed losses of $<0.2\%$ of the lithia content in 24 h at 900°C and $<0.6\%$ of the lithia in 24 h at 1000°C. In their study of the system Li_2O–TiO_2, Izquierdo and West (5) noted that loss of lithia by volatilization was not a serious problem for temperatures below ~ 1200°C.

0022-4596/98 $25.00

Diffraction Studies

Powder X-ray diffraction (PXRD) was used for the routine identification of phases in the equilibrated products and to provide intensity data for structure refinements by the Rietveld method (6). Samples for PXRD were prepared by grinding the reaction pellets in a tungsten carbide mill and back-pressing the powders into an aluminum sample holder. Measurements of diffracted intensities were made using a Philips 1050 goniometer with a PW1710 controller and using a long fine-focus copper tube operated at 40 kV and 40 mA. The diffractometer was configured with a 1°-divergent slit, 0.2-mm receiving slit, 1°-scatter slit, incident and diffracted beam Soller slits, and a diffracted-beam curved graphite monochromator. For the Rietveld refinements, intensity data were collected from 16° to 140° 2θ with a step size of 0.025°. The total counting time was typically 22 ks per run.

A powder neutron diffraction (PND) data collection was made on a cylindrical specimen composed of 1-cm diameter pressed pellets and weighing ~ 6 g. The sample was contained in a vanadium can. The data set was collected on the high-resolution powder diffractometer at the Australian Nuclear Science and Technology Organisation's research reactor. Intensity data was collected in the 2θ range 0.03 to 154.03°, at intervals of 0.05°, using a wavelength of 1.492 Å and a total counting time of 24 h.

Rietveld Refinements

Least squares refinements were carried out using the Rietveld program SR5, a local modification of the code by Hill and Howard (7) and Wiles and Young (8) which takes account of quantitative phase analysis of multiphase mixtures. Profile refinement parameters included a scale factor, two pseudo-Voigt shape parameters, a 2θ zero parameter, a three-term full-width at half-maximum function (9), calculated for nine half-widths on either side of the peak maxima, a peak asymmetry parameter for peaks less than 50° 2θ, and unit cell parameters. The background was modeled using a five-parameter polynomial fit. A similar refinement procedure was used for the PND data, except that a Voigt peak shape parameter was used. Scattering curves for ionised atoms were taken from *International Tables for X-ray Crystallography* (10). The neutron scattering lengths used were Li = − 0.190, Ti = − 0.344, O = 0.580, and Fe = 0.954×10^{-12} cm.

RESULTS AND DISCUSSION

Phase Studies

The results of the phase studies at 1000°C are presented in Fig. 1 as the ternary plot $LiO_{0.5}$-$FeO_{1.5}$-TiO_2. The new information obtained in this study concerns the characterisation of extensive ternary solid solutions based on the pseudobrookite-type and ramsdellite-type structures. Neither of these solid solutions were reported in the study by Yau and Hughes (1). Two three-phase fields were characterised, comprising ramsdellite(ss) + spinel(ss) + pseudobrookite(ss), and ramsdellite(ss) + pseudobrookite(ss) + rutile. The elemental atomic ratios and compositions of the phases comprising the 3-phase regions are given in Table 1.

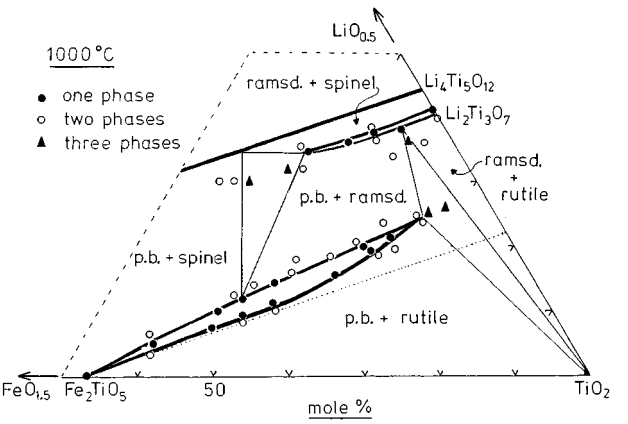

FIG. 1. Phase equilibria in the $LiO_{0.5}$-$FeO_{1.5}$-TiO_2 system (mol%) at 1000°C. p.b. = pseudobrookite(ss), ramsd. = ramsdellite(ss), spinel = spinel(ss). The dotted line corresponds to a stoichiometry of M_3O_5.

The most striking observation from an inspection of Fig. 1 is the relatively large departure of the pseudobrookite(ss) compositions from the M_3O_5 stoichiometric line given by the coupled substitution of $2Ti^{4+} + Li^{+}$ for $3Fe^{3+}$. The lower phase boundary in Fig. 1, where the pseudobrookite(ss) is in equilibrium with rutile, shows an increasing deviation from this line with increasing lithium content. Because of the substantial width of the single phase region, compositions at the upper phase boundary, in equilibrium with spinel(ss) or ramsdellite(ss), show a significantly greater deviation from stoichiometry to more metal-rich compositions than M_3O_5. The full range of the solid solution at 1000°C is from Fe_2TiO_5 to $Li_{0.77}Fe_{0.32}Ti_{2.07}O_5$.

In contrast to the behaviour of pseudobrookite(ss), the ramsdellite(ss) was found to have a narrow stoichiometry

TABLE 1
Phase Compositions in Three-Phase Regions at 1000°C

Phases present	Metal atom fractions [Li]	]Fe]	[Ti]	Composition
M_3O_5(ss)	0.125	0.400	0.475	$Li_{0.39}Fe_{1.24}Ti_{1.47}O_5$
+ spinel(ss)	0.350	0.285	0.365	$Li_{1.05}Fe_{0.85}Ti_{1.10}O_4$
+ ramsdellite(ss)	0.345	0.210	0.445	$Li_{2.00}Fe_{1.22}Ti_{2.58}O_8$
M_3O_5(ss)	0.245	0.100	0.655	$Li_{0.77}Fe_{0.32}Ti_{2.07}O_5$
+ ramsdellite(ss)	0.390	0.055	0.555	$Li_{2.25}Fe_{0.32}Ti_{3.20}O_8$
+ rutile	0.0	0.0	1.0	TiO_2

range and to approximately follow the compositional line corresponding to the substitution $3Fe^{3+} \leftrightarrow 2Ti^{4+} + Li^{+}$, as occurs for the spinel(ss) and rocksalt(ss) series (1). The lithium titanate end-member was prepared as a single phase at 41 mol% $LiO_{0.5}$. This is consistent with the phase study on the Li_2O-TiO_2 system by Mikkelsen, in which his Fig. 3 shows a homogeneity width from $\sim$40.5 to 42 mol% $LiO_{0.5}$ for the ramsdellite phase at 1000°C (11). The unit cell composition for the lithium titanate end member is $Li_{2.39}Ti_{3.40}O_8$. The limiting iron-containing ramsdellite composition at 1000°C incorporates 21 mol% $FeO_{1.5}$. The full range of the solid solution at 1000°C is from $Li_{2.39}Ti_{3.40}O_8$ to $Li_{2.00}Fe_{1.22}Ti_{2.58}O_8$. Note that the composition of the lithium titanate end-member is often expressed as $Li_2Ti_3O_7$. This gives an incorrect representation of the structural formula which is based on eight oxygens per unit cell. From a structure refinement, Morosin and Mikkelsen (12) have shown that the structural formula is $Li_{1.72}[Li_{0.57}Ti_{3.43}]O_8$, with lithium both substituting for titanium in the M_4O_8 octahedral framework and occupying sites in the 2×1 channels. This model was confirmed in a subsequent neutron diffraction study (13).

At 900°C the pseudobrookite(ss) showed the same large deviation from stoichiometry and a similar width to that measured at 1000°C. The solid solution is slightly more extended than at 1000°C, terminating at the composition $Li_{0.81}Fe_{0.27}Ti_{2.09}O_5$. The only significant change in the phase relations of the pseudobrookite(ss) at 900°C is that the two-phase region, pseudobrookite(ss) + spinel(ss), occurs over a much wider range of pseudobrookite(ss) compositions, $0.2 < [Fe]/\sum[M] < 0.67$, than at 1000°C, $0.4 < [Fe]/\sum[M] < 0.67$, where $[Fe]/\sum[M]$ is the atomic fraction of iron relative to the sum of the metal atoms, $M = Li + Fe + Ti$. The observed change is a result of the decreased stability of the ramsdellite(ss) at the lower temperature. As reported by Mikkelsen (11), the lithium titanate end-member ramsdellite phase is stable only above 940°C. Below 940°C it decomposes to $Li_4Ti_5O_{12}$ (spinel) plus rutile. At 900°C the lithium titanate is thus close to being stable and requires only a small free energy change to stabilise it. It appears from our study that such a factor is an increase in configurational entropy when iron is added as an extra cation. We found that a narrow region of iron-containing ramsdellite(ss) was stable at 900°C for compositions centred at $\sim$10 mol% $FeO_{1.5}$. However, the precise limits of the ramsdellite(ss) could not be determined because of the readiness with which phase fluctuations occurred on repeated heatings.

Helium Pycnometry Measurements

With regard to the pseudobrookite(ss), it is of prime interest to determine if the deviations from M_3O_5 stoichiometry shown in Fig. 1 are due predominantly to oxygen vacancies or to cation interstitials. In an attempt to resolve this issue, careful density measurements were made using a helium pycnometer applied to single-phase compositions with different Li:Fe:Ti atomic fractions. The measured densities are reported in Table 2, together with densities calculated for models based on anion vacancies and cation interstitials. The results give support to the interstitial cation model.

TABLE 2
Pycnometry Results for Pseudobrookite(ss) Phases

[Li]:[Fe]:[Ti] for pseudobrookite phase	Measured density (g/cm^3)	Calculated density (g/cm^3)
0.0:0.67:0.33 (Fe_2TiO_5)	4.33, 4.37	4.36
0.205:0.16:0.635	3.79, 3.82, 3.83	3.81 (cation interstitials) 3.69 (oxygen vacancies)
0.255:0.085:0.66	3.70, 3.67, 3.66	3.73 (cation interstitials) 3.53 (oxygen vacancies)

Based on an interstitial cation model, the pseudobrookite(ss) compositions can be obtained directly from the cation atomic fractions by normalising to five oxygens. The resulting compositions for single phases prepared during the phase equilibria study are reported in Table 3. The maximum deviation from stoichiometry corresponds to the composition $Li_{0.81}Fe_{0.27}Ti_{2.09}O_5 \equiv M_{3.17}O_5$.

Rietveld Refinement of PXRD Data

Pseudobrookite(ss). Rietveld refinements were made on PXRD data collected for single-phase pseudobrookite(ss)

TABLE 3
Unit Cell Parameters for Li-Pseudobrookite(ss) Phases

Atom fractions			Cell parameters (Å)			
[Li]	[Fe]	[Ti]	*a*	*b*	*c*	Composition
Compositions along upper phase boundary						
–	0.667	0.333	9.7933(1)	3.7299(1)	9.9756(1)	Fe_2TiO_5
0.050	0.555	0.395	9.7643(2)	3.7338(1)	9.9564(2)	$Li_{0.15}Fe_{1.68}Ti_{1.20}O_5$
0.100	0.445	0.455	9.7411(1)	3.7408(1)	9.9438(1)	$Li_{0.31}Fe_{1.37}Ti_{1.40}O_5$
0.120	0.400	0.480	9.7266(1)	3.7422(1)	9.9331(1)	$Li_{0.37}Fe_{1.23}Ti_{1.48}O_5$
0.145	0.345	0.510	9.7166(1)	3.7457(1)	9.9277(1)	$Li_{0.45}Fe_{1.07}Ti_{1.58}O_5$
0.185	0.250	0.565	9.6925(1)	3.7477(1)	9.9147(1)	$Li_{0.58}Fe_{0.78}Ti_{1.77}O_5$
0.200	0.200	0.600	9.6804(1)	3.7485(1)	9.9053(1)	$Li_{0.62}Fe_{0.62}Ti_{1.88}O_5$
0.255	0.085	0.660	9.6587(1)	3.7540(1)	9.8824(1)	$Li_{0.81}Fe_{0.27}Ti_{2.09}O_5$
Compositions along lower phase boundary						
0.035	0.565	0.400	9.7737(1)	3.7319(1)	9.9665(1)	$Li_{0.11}Fe_{1.70}Ti_{1.20}O_5$
0.070	0.465	0.465	9.7489(1)	3.7351(1)	9.9546(1)	$Li_{0.21}Fe_{1.40}Ti_{1.40}O_5$
0.110	0.365	0.525	9.7256(1)	3.7398(1)	9.9429(1)	$Li_{0.33}Fe_{1.10}Ti_{1.59}O_5$
0.155	0.260	0.585	9.6998(1)	3.7438(1)	9.9283(1)	$Li_{0.47}Fe_{0.79}Ti_{1.79}O_5$
0.180	0.220	0.600	9.6902(1)	3.7458(1)	9.9204(1)	$Li_{0.55}Fe_{0.68}Ti_{1.85}O_5$
0.205	0.160	0.635	9.6714(1)	3.7479(1)	9.9023(1)	$Li_{0.64}Fe_{0.50}Ti_{1.97}O_5$

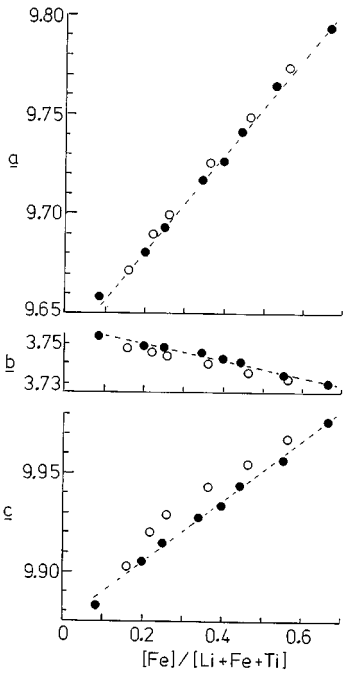

FIG. 2. Unit cell parameters as a function of [Fe]/[Fe + Ti + Li] atomic fraction for the pseudobrookite(ss). Filled and open circles correspond to compositions along the upper and lower phase boundaries in Fig. 1.

compositions lying along both the upper and lower phase boundaries. The refined unit cell parameters are given in Table 3 and plotted as a function of $[Fe]/\sum[M]$, in Fig. 2. The order of unit cell parameters, $a \sim 9.7$, $b \sim 3.7$, $c \sim 9.9$ Å, corresponds to the space group setting C*cmm*, consistent with our previous studies on pseudobrookite-related solid solutions (14, 15). With increasing substitution of Li + Ti for Fe the *a* and *c* parameters both decrease linearly while the *b* parameter undergoes a small increase. The changes in unit cell parameters result in an overall decrease in unit cell volume with decreasing $[Fe]/\sum[M]$. Between Fe_2TiO_5 and the solid solution limit, $Li_{0.81}Fe_{0.27}Ti_{2.09}O_5$, the volume reduction is 1.7%. A comparison of the filled and open circles in Fig. 2 shows that the *c* parameter is most strongly affected by stoichiometry variations. Increasing substitution of lithium for titanium at constant $[Fe]/\sum[M]$ is seen to result in a contraction along *c*, a smaller contraction along *a*, and an expansion along *b*. There is an overall contraction in unit cell volume accompanying the substitution of lithium for the smaller titanium atom which can be explained by lithium occupying interstitial sites. This was verified by neutron diffraction studies as will be discussed below.

Refined structural parameters for selected pseudobrookite(ss) compositions covering the complete solid solution range are presented in Table 4. The Rietveld refinements gave unambiguous evidence for the selective ordering of lithium in the four-fold M1 sites. When Ti scattering curves were used for both M1 and M2 sites, the refined site occupancy for M2 corresponded to full occupancy or slightly higher (due to Fe substitution in M2) at all compositions, whereas the site occupancy for M1 decreased monotonically with increasing lithium content. The results are presented in Table 4 in the form of mean atomic number (m.a.n.) of the M1 site (16), which decreases from a value of 22.7 for Fe_2TiO_5 to a value of 10.2 for $Li_{0.81}Fe_{0.27}Ti_{2.09}O_5$. The refined m.a.n. values for the M1 site are in good agreement with values calculated from the phase compositions assuming M2 contains only titanium and iron and M1 contains iron and lithium.

TABLE 4
Rietveld Refinement Results for Pseudobrookite(ss) Phases

[Li]:[Fe]:[Ti] atom fractions	0.0:0.67:0.33	0.125:0.41:0.465	0.20:0.20:0.60	0.255:0.085:0.66
a (Å)	9.7933(1)	9.7305(1)	9.6804(2)	9.6591(1)
b (Å)	3.7299(1)	3.7430(1)	3.7485(1)	3.7535(1)
c (Å)	9.9757(1)	9.9350(1)	9.9053(2)	9.8829(1)
M1 (*x*, 0, 1/4)				
x	0.8131(2)	0.8119(3)	0.8071(3)	0.8040(3)
B (Å^2)	0.5	0.5	0.5	0.5
m.a.n[a]	22.7(1)	18.5(1)	13.5(1)	10.2(1)
M2 (*x*, 0, *z*)				
x	0.1366(1)	0.1361(2)	0.1354(2)	0.1355(1)
z	0.0641(1)	0.0638(2)	0.0653(2)	0.0652(1)
B (Å^2)	0.42(2)	0.61(3)	0.50(4)	0.60(2)
O1 (*x*, 0, 1/4)				
x	0.2367(8)	0.2321(8)	0.2246(6)	0.2221(5)
B (Å^2)	2.19(7)	2.10(9)	1.42(8)	1.04(4)
O2 (*x*, 0, *z*)				
x	0.0481(5)	0.0448(6)	0.0468(5)	0.0471(4)
z	0.8858(5)	0.8817(5)	0.8840(4)	0.8841(3)
B (Å^2)	2.19(7)	2.10(9)	1.42(8)	1.04(4)
O3 (*x*, 0, 1/4)				
x	0.3142(5)	0.3147(5)	0.3146(6)	0.3155(3)
z	0.9273(5)	0.9302(6)	0.9368(5)	0.9390(4)
B (Å^2)	2.19(7)	2.10(9)	1.42(8)	1.04(4)
R_{wp} (%)	15.1	18.8	14.3	14.9
R_b (%)	4.5	6.1	3.8	5.5

[a]m.a.n. = mean atomic number at site, defined in Ref. (16).

The results in Table 4 show that the main structural changes accompanying substitution of Li + Ti for Fe in the pseudobrookite(ss) are parallel displacements along [100] of M1 and O1 which both lie on the (001) mirror planes at $z = \pm 1/4$, and displacement of O3 along [001]. These displacements are illustrated in a [010] projection of the structure in Fig. 3. In this diagram we have represented the coordination polyhedron for M1 as a bi-capped tetrahedron rather than as a highly distorted octahedron. When presented in this way, a different perspective is gained of the structure as comprising (001) stepped layers of edge-shared octahedra containing M2, which are connected via corner-sharing with M1 tetrahedra. The diagram also shows that

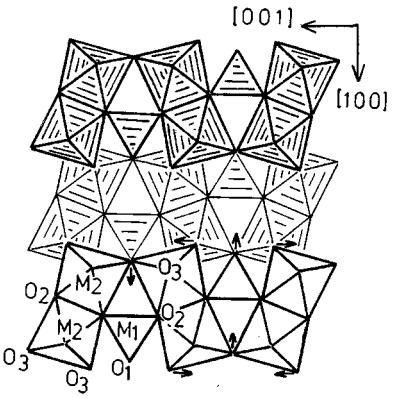

FIG. 3. Polyhedral representation of the pseudobrookite structure, in projection along [010]. Arrows show main atomic movements (exaggerated) resulting from substitution of Li + Ti for Fe.

the main interstitial volume is centred on the mirror planes at $z = \pm 1/4$. The oxygen displacements shown in Fig. 3 correspond to cooperative rotation of pairs of edge-shared octahedra containing M2 in the (001) layers. This allows the M1 site volume to expand to accomodate increasing lithium contents, even though the overall unit cell contracts.

Ramsdellite(ss). Rietveld refinement results for different single-phase ramsdellite(ss) compositions are given in Table 5. The published coordinates from a neutron diffraction refinement of $Li_2Ti_3O_7$ in space group P*nma* (13) were used as starting parameters for the refinements. The analysed phase compositions were used to allocate Ti + Fe to the framework metal atom site, with Li added to complete the occupation, and with the remaining lithium distributed over two interstitial sites in the channels. The parameters for the partially occupied lithium sites from Ref. (13) were held fixed in the refinements.

TABLE 5
Rietveld Refinement Results for Ramsdellite(ss) Phases[a]

[Li]:[Fe]:[Ti] atom fractions	0.40:0.0:0.60	0.36:0.14:0.50	0.34:0.21:0.45
a (Å)	9.5505(1)	9.5873(2)	9.5966(1)
b (Å)	2.9453(1)	2.9502(1)	2.9514(1)
c (Å)	5.0164(1)	5.0054(1)	5.0003(1)
M1			
(*x*, 1/4, *z*)			
occupancy	0.14Li + 0.86Ti	0.08Li + 0.20Fe + 0.72Ti	0.05Li + 0.30Fe + 0.65Ti
x	0.1394(1)	0.1405(1)	0.1417(1)
z	0.9680(2)	0.9756(3)	0.9800(2)
B (Å^2)	0.98(3)	0.76(3)	0.38(2)
O1			
(*x*, 1/4, *z*)			
x	0.2736(3)	0.2772(4)	0.2792(4)
z	0.6712(8)	0.6882(9)	0.6990(8)
B (Å^2)	1.35(9)	1.31(10)	1.17(9)
O2			
(*x*, 1/4, *z*)			
x	0.9662(4)	0.9646(4)	0.9626(4)
z	0.2023(6)	0.2025(8)	0.2087(7)
B (Å^2)	1.17(8)	1.18(10)	1.00(9)
R_{wp} (%)	15.9	17.6	15.3
R_b (%)	5.4	5.2	4.9

[a]Li1 at 0.445, 0.181, 0.942 and Li2 at 0.047, 1/4, 0.540, from Ref. (13); fixed during refinement.

The results in Table 5 show that replacement of Ti + Li by Fe in the ramsdellite structure results in small expansions of the *a* and *b* cell parameters and a contraction in *c*. Overall the unit cell expands by 0.3% from $Li_{2.39}Ti_{3.40}O_8$ to $Li_{2.04}Fe_{1.16}Ti_{2.62}O_8$. The main structural changes involve displacements of M and O1 along [001]. These displacements, together with the anisotropic unit cell parameter changes, reflect a progressive flattening of the (010) layers of octahedra by rotation of the double chains of octahedra about their corner linkages, as iron is substituted into the structure.

Location of Interstitial Lithium Atoms in $Li_{0.81}Fe_{0.27}Ti_{2.09}O_5$

The Rietveld refinements of PXRD data were unable to provide information on the location of the extra lithium atoms in the lithia-rich nonstoichiometric pseudobrookite(ss) phases. In an attempt to locate the interstitial atoms a powder neutron diffraction data set was collected on the most lithia-rich composition, $Li_{0.81}Fe_{0.27}Ti_{2.09}O_5$. Starting coordinates for the M1, M2, and O1–O3 oxygen sites were obtained from the PXRD refinement. On convergence of the refinement a difference Fourier map was generated which revealed a partially occupied interstitial site in the mirror plane at $z = \pm 1/4$. The peak in the difference Fourier map was negative, consistent with the interstitial atom being lithium or titanium, while the bond lengths to oxygen corresponded more closely to Li–O distances. Lithium was added at this site and its site occupancy refined, giving excellent agreement with the occupancy expected from the analysed excess lithium (0.17 excess Li per M_3O_5). Due to almost complete cancelling of scattering from iron (positive scattering length) and lithium/titanium (negative scattering lengths) in the M1 site the scattering contribution from this site was very small. The coordinates and isotropic displacement parameter for M1 were held fixed during the refinement. The final refinement with the interstitial lithium included and using anisotropic displacement parameters for M2 and O1–O3 converged at $R_{wp} = 4.8\%$, $R_B = 1.0\%$. The refinement results are reported in Table 6.

The interstitial lithium occupies a five-coordinated site with square pyramidal geometry. This coordination is commonly adopted by lithium, for example in Li-inserted anatase and TiO_2(B) (17, 18). The LiO_5 polyhedron shares faces with $M1O_6$ octahedra along [010], giving short Li-M1 distances of 2.3 Å. A similar face-sharing of interstitial LiO_4 polyhedra and framework (Ti, Li)O_6 octahedra, with

TABLE 6
Rietveld Refinement of Neutron Diffraction Data for $Li_{0.81}Fe_{0.27}Ti_{2.09}O_5$

Composition: $Li_{0.81}Fe_{0.27}Ti_{2.09}O_5$
Unit Cell: C*cmm*, $a = 9.6576(2)$, $b = 3.7532(1)$, $c = 9.8820(2)$ Å
Refinement: $2\theta = 12$–153°, 253 reflections, 40 variables
$R_{wp} = 4.8\%$, $R_B = 1.0\%$

Atom	*x*	*y*	*z*	B (Å^2)	Scattering length ($\times 10^{-12}$ cm)
M1[a]	0.8041	0	1/4	0.5	−0.042(2)
M2	0.1352(2)	0	0.0646(3)	0.61(6)	−0.269(3)
Li	0.445(4)	0	1/4	1.0	−0.028(3)
O1	0.2222(2)	0	1/4	0.62(2)	
O2	0.0461(1)	0	0.8845(1)	0.97(2)	
O3	0.3149(1)	0	0.9398(1)	0.64(2)	
	B_{11}	B_{22}	B_{33}	B_{13}	
M2	0.24(9)	0.32(9)	0.63(9)	0.02(2)	
O1	0.79(8)	1.18(7)	0.39(6)	0.0	
O2	0.39(5)	2.05(6)	0.47(4)	0.01(1)	
O3	0.63(5)	0.33(4)	0.87(5)	0.01(1)	

[a]Coordinates and B for M1 fixed at values from PXRD refinement.

Li-M = 2.33 Å, occurs in $Li_2Ti_3O_7$ (13). The M1 site in $Li_{0.81}Fe_{0.27}Ti_{2.09}O_5$ has almost 2/3 occupancy by lithium. We propose that the interstitial site is occupied only when the adjacent M1 sites are occupied by lithium. This gives rise to Li_3 clusters with Li-Li = 2.3 Å. This situation is illustrated in Fig. 4. Similar short Li-Li separations, Li-Li = 2.2–2.3 Å, occur in Li_2O (19) and in a number of lithium-rich metal oxides such as Li_5GaO_4 (20). Long-range ordering of lithium and iron/titanium in the M1 sites, as illustrated in Fig. 4, would give rise to a $3\times$ superstructure along **g**(010), or to diffuse intensity in (010) layers at $n/3 \times$ **g**(010), if the ordering is confined to individual [010] chains only. We plan to investigate this aspect from studies on single-crystal preparations.

The refined scattering lengths at the M1, M2 and interstitial sites were $-0.042(2)$, $-0.269(3)$, and $-0.028(3) \times 10^{-12}$ cm. Using the reasonable assumption that only the small cations Ti^{4+} and Fe^{3+} occupy M2, the scattering length for M2 can be used in conjunction with the phase composition, $Li_{0.81}Fe_{0.27}Ti_{2.09}O_5$, to calculate the occupancies of the three sites. This gives a structural formula $(Li)_{0.17}[Fe_{0.16}Ti_{0.20}Li_{0.64}]$ $\{Fe_{0.11}Ti_{1.89}\}$ O_5, where ( ) [ ], and { } refer to interstitial, M1, and M2 sites. The calculated scattering cross sections for the M1 and interstitial sites, based on this formula are -0.039 and -0.032×10^{-12} cm, which are in good agreement with the refined values. The site assignments can be further checked using bond length/bond strength calculations (21). Based on the above assignments the formal valence sums at M1 and M2 are 1.92 and 3.94 and these compare closely with the

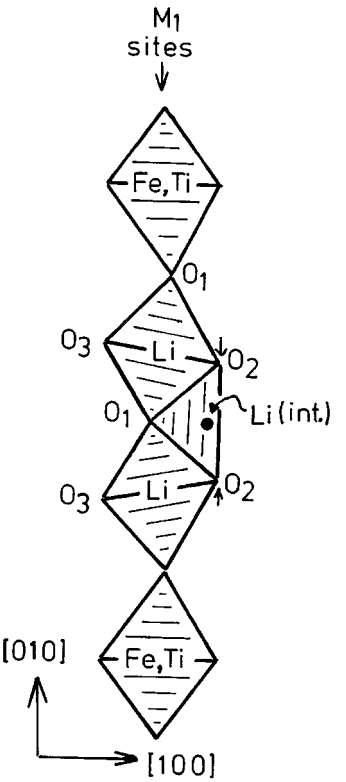

FIG. 4. Proposed model for incorporation of lithium in square-pyramidal interstitial sites in Li-pseudobrookite, forming local Li_3 clusters. Arrows show local movements of O2 atoms, consistent with refined anisotropic displacement parameters.

corresponding values calculated from the refined bond lengths of 1.90 and 3.89, respectively.

Polyhedral bond lengths and angles for $Li_{0.81}Fe_{0.27}Ti_{2.09}O_5$ are given in Table 7. The M1–O_6 polyhedron is an extremely deformed octahedron which is probably better described as a bicapped tetrahedron. The mean deviation of bond angles from 109.5° for the M1-$(O1, O2)_4$ tetrahedron is 10.0°, compared with a larger mean deviation of the angles in M1-$(O1, O2, O3)_6$ from ideal octahedral values of 16.2°. In Fig. 2 the coordination polyhedra for M1 are shown as tetrahedra rather than as the usually depicted octahedra. The Li-O2 bond lengths are longer than commonly reported for five-coordinated lithium. However, as seen in Table 6, O2 has a large anisotropic displacement parameter B_{22}, corresponding to a r.m.s. displacement along [010] of 0.16 Å. This would be consistent with the O2 atoms moving towards the interstitial site when it is occupied, and away from it when it is empty, thus decreasing the interstitial Li-O2 distances from the average value obtained in the refinement. The local changes in the O2 positions, in response to lithium in interstitial sites, is illustrated in Fig. 4.

The mean M1-O and M2-O bond lengths, polyhedral volumes, and associated distortion indices (15) for $Li_{0.81}Fe_{0.27}Ti_{2.09}O_5$ are compared with the corresponding

TABLE 7
Polyhedral Bond Lengths (Å) and Angles (°) for $Li_{0.81}Fe_{0.27}Ti_{2.09}O_5$

Distances		Angles		
M1-O2 (×2)	1.965(2)	85.3(1)		
M1-O1 (×2)	2.036(1)	106.66(4) (×4)	134.1(1)	
M1-O3 (×2)	2.200 (1)	164.24(9) (×2)	78.22(4) (×4)	116.82(8)
		78.94(4) (×2)		
⟨M1-O⟩	2.067	O2	O1	O3
M2-O2	1.822(2)			
M2-O3 (×2)	1.938(1)	104.19(7) (×2)	151.1(1)	
M2-O2	1.977(4)	80.2(1)	95.0(1) (×2)	
M2-O1	2.015(4)	98.6(2)	85.2(1) (×2)	178.85(8)
M2-O3	2.130(3)	160.6(2)	77.56(8) (×2)	80.40(6) 100.8(1)
⟨M2-O⟩	1.970	O2	O3	O2 O1
Li-O1	2.15(4)			
Li-O2 (×4)	2.30(2)	92.8(9) (×4)	70.51(6) (×2)	
			109.2(1) (×2)	
⟨Li-O⟩	2.27	O1	O2	
Li-M1	2.32(2)	Li-M2	3.20(2)	M1-M2 3.090(3)
M2-M2	2.907(5)			

TABLE 8
Cation Bond Valences, Polyhedral Volumes for MO_6 and Distortion Indices[a]

	$Li_{0.81}Fe_{0.27}Ti_{2.09}O_5$	Fe_2TiO_5[b]
M1	0.64Li + 0.16Fe + 0.20Ti	0.67Fe + 0.33Ti
Calc. bond valence	1.90	3.12
Formal bond valence	1.92	3.33
Polyhedral volume (Å^3)	10.40	10.01
Polyhedral distortion	0.038	0.028
M2	0.05Fe + 0.95Ti	0.67Fe + 0.33Ti
Calc. bond valence	3.89	3.66
Formal bond valence	3.94	3.33
Polyhedral volume (Å^3)	9.73	10.13
Polyhedral distortion	0.014	0.016
Cell volume (Å^3)	358.2	364.8
Polyhedral volume (Å^3)	119.4	121.1
Interstitial volume (Å^3)	238.8	243.8

[a]Definitions given in Ref. (15).
[b]Results for Fe_2TiO_5 calculated from data in Ref. (22).

values for Fe_2TiO_5 in Table 8. The results for Fe_2TiO_5 are from the single crystal refinement of Tiedemann and Muller-Buschbaum (22) who reported a statistical distribution of 2/3Fe + 1/3Ti in M1 and M2. Note, however, from the bond valence calculations for Fe_2TiO_5 that the refinement results (22) are consistent with partial ordering of titanium in the M2 site. Due to the high degree of ordering of Ti in M2 and Li in M1 in the Li-pseudobrookites, the substitution of Li + Ti for Fe in Fe_2TiO_5 results in expansion of M1-O distances and a contraction of M2-O distances. The reduction in the M2-O_6 polyhedral volume is comparable with the increase in the M1-O_6 volume and, since there are twice as many of the former polyhedra, there is an overall decrease in the unit cell volume. However, as seen from the results in Table 8, the major contributor to the decreased volume for the Li-pseudobrookite is the reduction in interstitial volume as the oxygen framework contracts to satisfy the coordination requirements of the interstitial lithium atoms.

Application to Ilmenite Upgrading

M_3O_5 phases with the pseudobrookite structure are soluble in concentrated sulphuric acid and so they are suitable feedstocks to the sulphate-route process for titania pigment production (23). The major commercial production of acid-soluble M_3O_5 for pigment plant feedstocks is by electrosmelting ilmenite at high temperature. The titania slags thus produced are preferred to ilmenite as pigment plant feedstocks because they are high in titania (75–85% wt % TiO_2) and so there are lower volumes of waste products to dispose of. However, slag production is a very energy intensive and expensive process. The results presented here show that Li-pseudobrookite phases containing more than 80 wt% TiO_2 can be produced by relatively low temperature reactions in air. Suitable natural starting materials for production of lithium-substituted M_3O_5 would be secondary ilmenites and leucoxenes which, without treatment, are not acid soluble.

The viability of an upgrading process using lithium additives will be limited by the high cost of lithium compounds. Preferably the lithium would need to be recouped and re-used. This may be achievable by ion exchange of lithium by protons (24), or by low temperature exchange reactions of the type $2Li^+ \leftrightarrow M^{2+}$ + vacancy (25). We are currently pursuing studies along these lines.

ACKNOWLEDGMENTS

We thank Margaret Elcombe and Brett Hunter at the Australian Nuclear Science and Technology Organisation for collecting the neutron diffraction data set and Bob Roth for initiating the project during a visit to the Division.

REFERENCES

1. Y-C. Yau and J. M. Hughes, *J. Amer. Ceram. Soc.* **66,** 479 (1983).
2. A. J. Easteal and D. J. Udy, *J. Appl. Chem. Biotechnol.* **23,** 865 (1973).
3. R. C. Peterson and I. E. Grey, *Can. Mineral.* **33,** 1083 (1995).
4. I. E. Grey, L. M. D. Cranswick, C. Li, L. A. Bursill, and J. L. Peng, *J. Solid State Chem.* **138,** 74 (1998).
5. G. Izquierdo and A. R. West, *Mat. Res. Bull.* **15,** 1655 (1980).
6. H. M. Rietveld, *J. Appl. Crystallogr.* **2,** 65 (1969).
7. R. J. Hill and C. J. Howard, *J. Appl. Crystallogr.* **18,** 173 (1985).
8. D. B. Wiles and R. A. Young, *J. Appl. Crystallogr.* **14,** 149 (1981).
9. G. Cagliotti, A. Paoletti, and F. P. Ricci, *Nucl. Instrum.* **3,** 223 (1958).
10. "International Tables for X-ray Crystallography," Vol. IV, Kynoch, Birmingham, UK, 1974.

11. J. C. Mikkelsen Jr., *J. Am. Ceram. Soc.* **63,** 331 (1980).
12. B. Morosin and J. C. Mikkelsen Jr., *Acta Crystallogr. B* **35,** 798 (1979).
13. I. Abraham, P. G. Bruce, W. I. F. David, and A. R. West, *J. Solid State Chem.* **78,** 170 (1989).
14. I. E. Grey and J. Ward, *J. Solid State Chem.* **7,** 300 (1973).
15. I. E. Grey, C. Li, and I. C. Madsen, *J. Solid State Chem.* **113,** 62 (1994).
16. M. F. Brigatti, S. Contini, S. Capedri, and L. Poppi, *Eur. J. Mineral.* **5,** 73 (1993).
17. G. Nuspl, K. Yoshizawa, and T. Yamabe, *J. Mater. Chem.* **7,** 2529 (1997).
18. R. J. Cava, D. W. Murphy, S. Zahurak, A. Santoro, and R. S. Roth, *J. Solid State Chem.* **53,** 64 (1984).
19. E. Zintl, A. Harder, and B. Dauth, *Z. Electrochem.* **40,** 588 (1934).
20. F. Stewner and R. Hoppe, *Z. Anorg. Allgem. Chem.* **381,** 140 (1971).
21. I. D. Brown and K. K. Wu, *Acta Crystallogr. B* **32,** 1957 (1976).
22. P. Tiedemann and H. Muller-Buschbaum, *Z. Anorg. Allgem. Chem.* **494,** 98 (1982).
23. I. E. Grey, *Chem. Austral.* **59,** 158 (1992).
24. A. Le Bail and J. L. Fourquet, *Mat. Res. Bull.* **27,** 75 (1992).
25. J. C. Joubert, *Bull. Soc. Fr. Mineral. Crystallogr.* **90,** 598 (1967).